SKB

TECHNICAL REPORT 89-29

Interim report on the settlement test in Stripa

Lennart Börgesson, Roland Pusch
Clay Technology AB, Lund

November 1989

SVENSK KÄRNBRÄNSLEHANTERING AB
SWEDISH NUCLEAR FUEL AND WASTE MANAGEMENT CO
BOX 5864 S-102 48 STOCKHOLM
TEL 08-665 28 00 TELEX 13108-SKB

INTERIM REPORT ON THE SETTLEMENT TEST IN STRIPA

Lennart Börgesson, Roland Pusch

Clay Technology AB, Lund

November 1989

INTERIM REPORT ON THE SETTLEMENT TEST IN STRIPA

Lennart Börgesson
Roland Pusch

Clay Technology AB
Lund, Sweden

CONTENTS Page

SUMMARY

A deposition hole, of the KBS 3 concept type, is being simulated by a borehole with 40 cm diameter in the Stripa mine. The canister is heated and different vertical loads applied to the canister. The resulting canister displacement, rock displacements and swelling and compression of the compacted bentonite and sand/bentonite overfill are studied.

The test is still running. So far the results and calculations have yielded the following main conclusions:

1. The canister is heaving since the compacted bentonite is swelling upwards, thereby compacting the overlying sand/bentonite overfill.

2. The effect of a temperature increase on the surrounding rock can only be explained by block movements. The very high pore pressure induced in heated bentonite is strongly affecting the rock.

3. The total consolidation settlement caused by the weight of the canister is several times larger than the total creep settlement achieved in the initial 100-1 000 years.

4. The processes observed during the test are fairly well understood and seems to be predictable.

The report ends up with a suggestion of how to continue and finish the test, and with a prediction of the result of an increased canister load at the present high temperature.

PREFACE

This investigation is a part of the Swedish R & D for final disposal of nuclear waste which is being financed by SKB. Most of the practical work work has been carried out by the personnel of Stripa Mine Service and Clay Technology AB.

The drawings not produced by the computer were drawn by Birgitta Hellström and the manuscript was edited by Irene Hansen.

The support from Anders Bergström, SKB, offered through numerous fruitful discussions, and the contributions from all other persons which in various way have been involved in the project are highly appreciated.

SYMBOLS

c = specific heat

c_p = coefficient of consolidation at constant volume

c_{sv} = coefficient of swelling at constant stress

c_v = coefficient of consolidation at constant stress

D_w = coefficient of water diffusion

E = Young's modulus

e = void ratio

F = force

K = coefficient of earth pressure

p = average stress

p_x, p_z = vertical pressure

q = deviatoric stress

r = radius

w = water ratio

α = coefficient of thermal expansion

δ = displacement

ε = strain

λ = coefficient of thermal conductivity

ρ = bulk density

ρ_d = dry density

ρ_m = density at saturation

ρ_s = particle density

ρ_w = density of pore water

σ_1 = major principal stress

σ_3 = minor principal stress

σ_s = swelling pressure

ϕ = friction angle

1. INTRODUCTION

The settlement and heave of a canister embedded in highly compacted bentonite, according to the KBS 3 concept, has been measured in a simulated deposition hole in Stripa. The purpose of the test is to study the movement of a canister in a deposition hole caused by canister weight, consolidation and swelling of the bentonite, and heating or cooling.

2. TEST ARRANGEMENT

The test is carried out in the Full Scale Drift in Stripa mine in hole H10 which was used for high temperature heater tests by LBL. The test area and rock characteristics are described in the LBL reports termed SAC 21, 35 and 38. Several boreholes originating from earlier studies and located close to H10 have been used for various purposes in the present test.

Hole H10 is 406 mm in diameter and 5.5 m deep. Below 3.0 m depth the hole is plugged with concrete supported by a very rigid set of rails. The arrangement in the 3.0 m deep test section of the "deposition" hole is shown in Fig 1. The 100 cm long steel cylinder representing a canister with a diameter of 20.0 cm, is equipped with an exchangable heater. The cylinder is surrounded by blocks of compacted bentonite which will yield a final density at saturation of ρ_m=1.99 t/m^3, assuming only radial redistribution of water and clay. The upper part of the hole is filled with a mixture of 10% bentonite and 90% sand. The density of that mixture was not determined with any accuracy but since only little compaction effort was made it is assumed that the density is ρ_m=2.1 t/m^3 (dry density ρ_d=1.75 t/m^3 corresponding to 85% degree of modified Proctor compaction). The uppermost part of the hole was sealed by a concrete plug preventing upward movement of the clay materials in the hole.

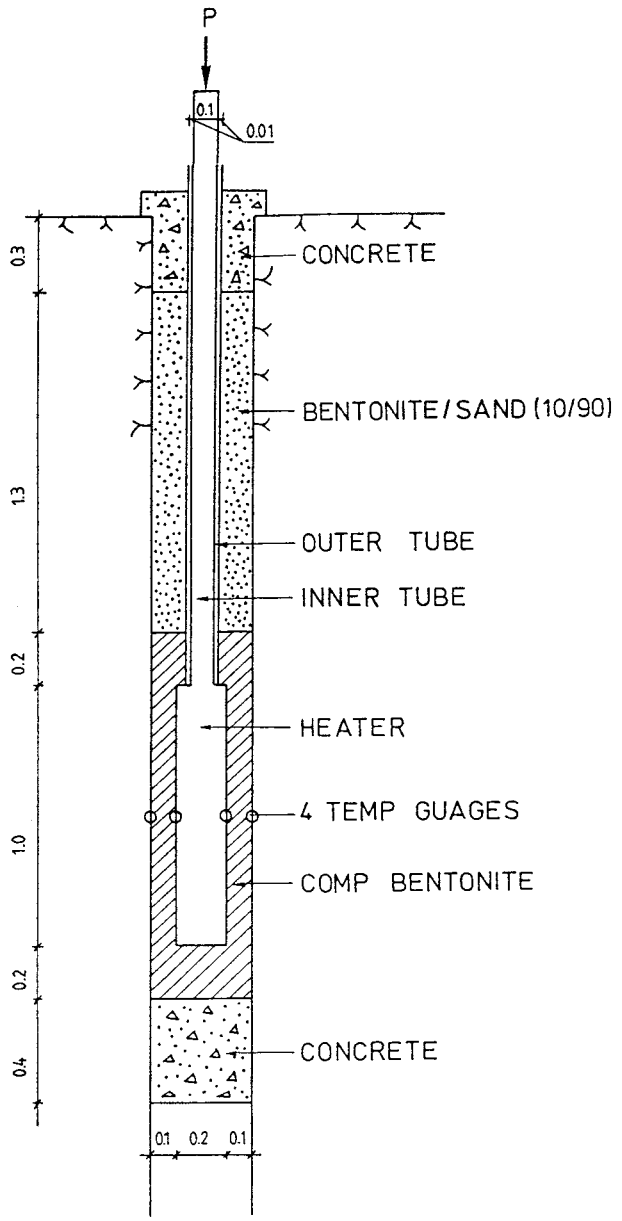

Fig 1. The simulated deposition hole.

The simulated weight of the cylinder was transferred through the buffer and concrete by an inner tube which ran friction-free through a fixed outer tube. The load on the cylinder was obtained by loading the outer end of a lever arm as shown in Fig 2.

Four temperature gauges were installed, two at the rock wall in the hole and two at the heater clay interface at mid-height of the cylinder, which will be termed "heater" hereafter.

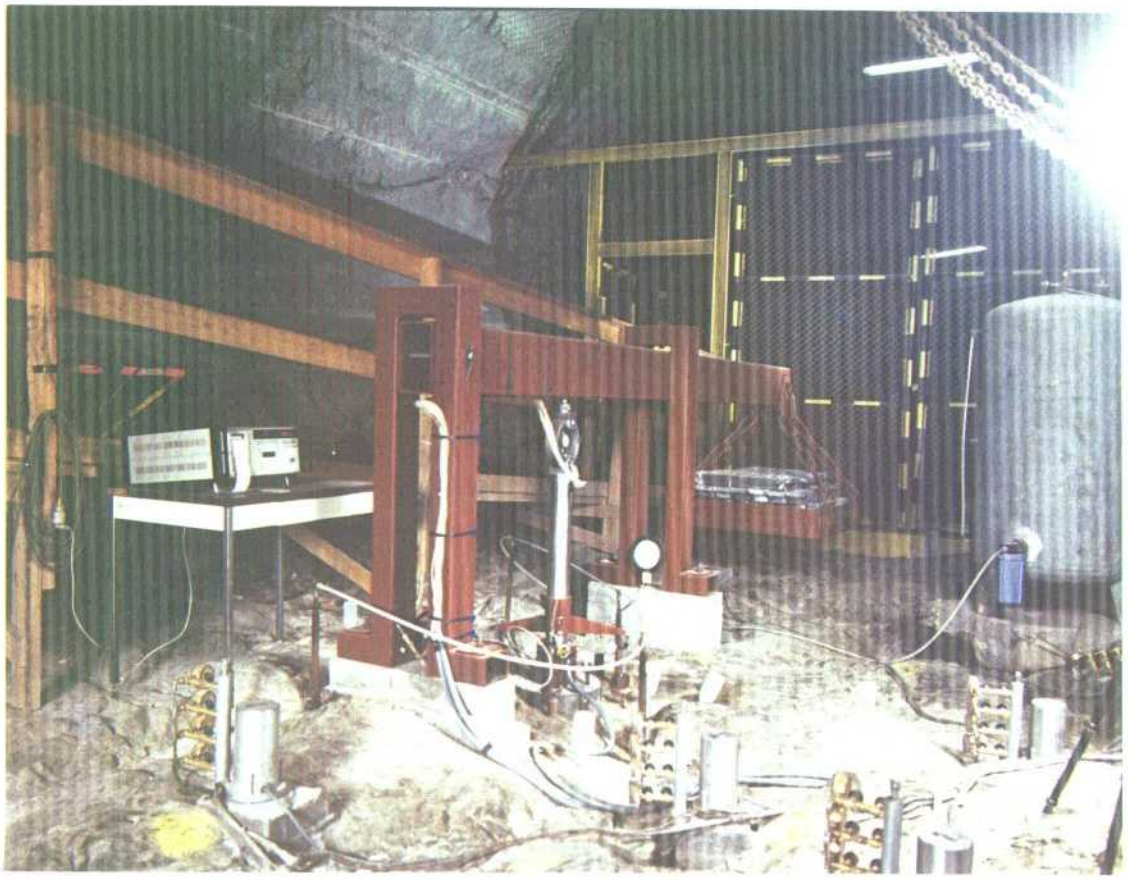

Fig 2. Photo of the arrangement

The vertical displacement of the heater was measured by four deformation gauges, while vertical movements of the floor was measured at regular intervals by use of precision levelling of 8 dowels installed before the heat was switched on. These measuring points are shown in Fig 3.

The heater hole is surrounded by many boreholes used for different measurements during the LBL tests and these holes drain the floor, i.e. prevent build-up of high water pressures around the heater hole. However, keeping them water-filled ensured water saturation of the clay in the heater hole.

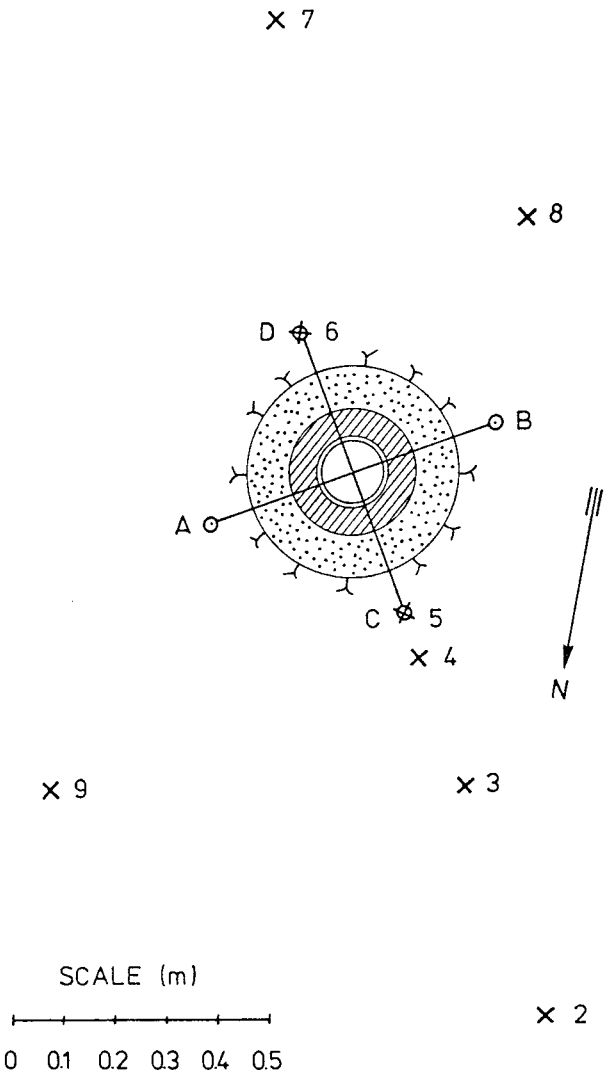

Fig 3. Location of points for measurement of vertical displacements.
o Dial gauges for canister displacements
x Dowels for rock displacement recording

The swelling pressure in the saturated clay is estimated at $\sigma_s \approx 4$ MPa at $\rho_m = 1.99$ t/m^3. Since the area of the base of the heater on which the swelling pressure acts is larger than the top area, due to the shaft, a vertical load had to be applied in order to balance the upward force. Since the shaft of the heater is 10 cm in diameter the resulting force at saturation amounts to $\Delta F \approx 3.14$ t.

3. TEST PROGRAM AND TEST RESULTS

The test started on June 11, 1986. During the first 9 months the lever arm was fixed in the vertical direction and the force measured by a force transducer at the top of the heater shaft. Due to the elasticity of the system some vertical displacement was recorded. On November 20, 1986 the first external load was applied and on March 15, 1987, the lever arm was released. The vertical force on the heater shaft was 2.7 t before and 4.05 t after release of the lever arm due to an additional external load of 545 kg on the lever arm. The load was then increased stepwise until December 17, 1987, when the total force on the heater shaft was 7.52 t. On August 31, 1988, the heater was switched on, giving a power of 660 W. It was decreased to 600 W two weeks later since the temperature approached 100°C at the surface of the heater, i.e. the upper limit that had been set beforehand.

The movement of the canister measured by transducers A and B as a function of time from the start of the test is shown in Fig 4, which also shows the applied loads. The graph shows that an increase of the load initially yields settlement, but after some time the settlement is successively transformed into heave even at the load 7.52 t, which is more than twice the calculated load needed to balance the upward force. The reason for this is discussed in Chapter 4.

The applied heat resulted in a significant heave which is shown as a displacement of the canister in Fig. 4. Primarily, the heave was caused by the thermal expansion of the steel cylinder and shaft. The heave continued at a slow rate even a year after the start of the heating period.

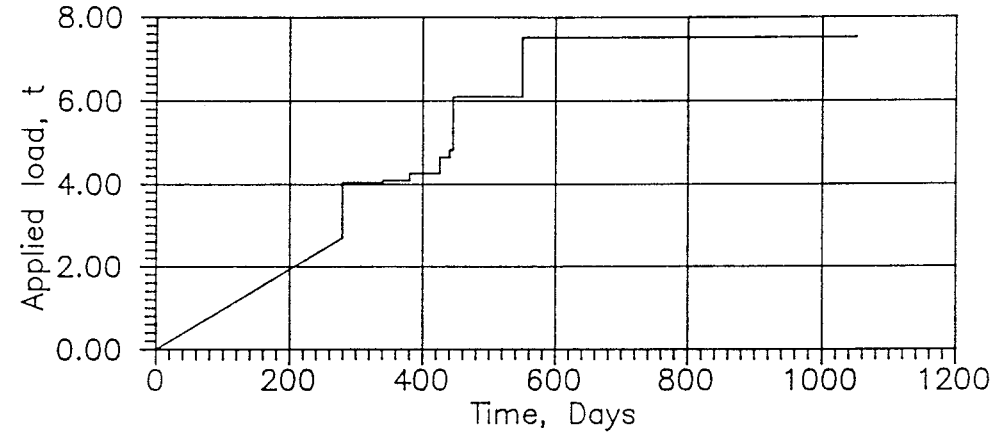

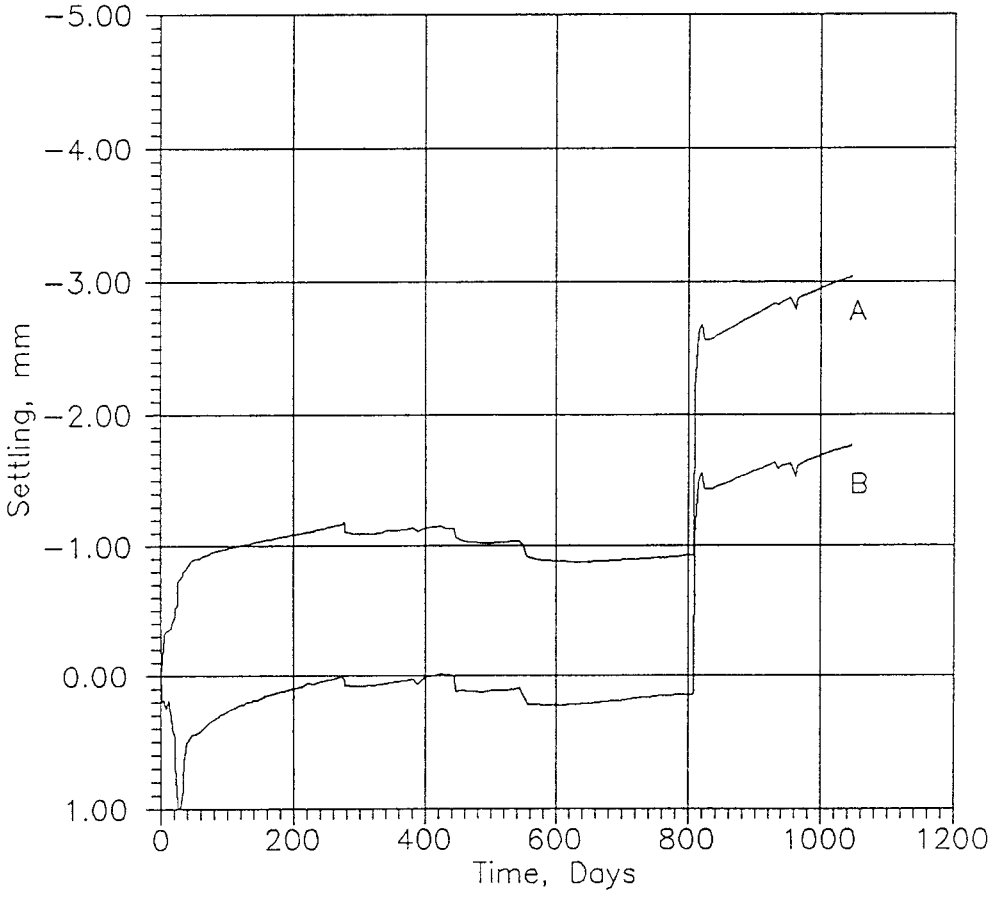

Fig 4. Canister displacements measured by gauges A and B. + means settlement. - means heave.

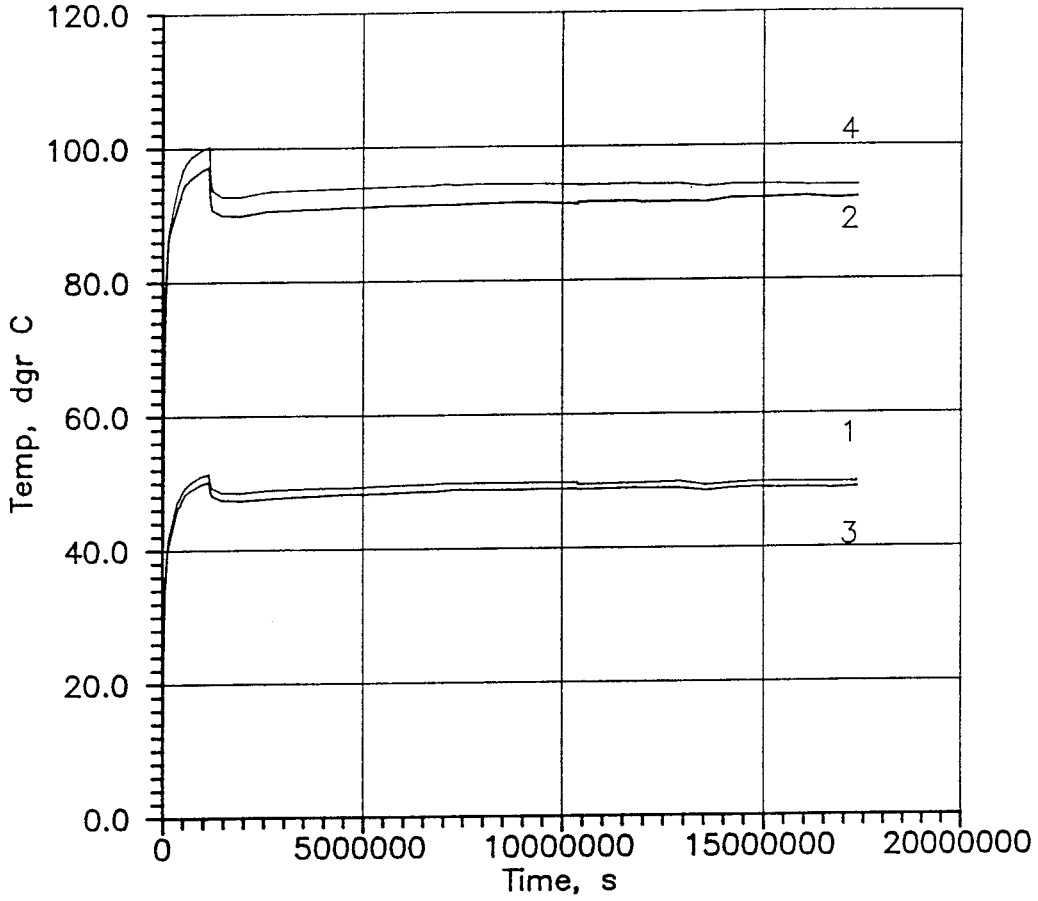

Fig 5. Measured temperature at the bentonite/canister surface (2, 4) and at the bentonite/rock surface (1, 3).

The temperatures measured at the canister surface and at the rock surface are shown in Fig 5. After about 2 months ($5.2 \cdot 10^6$ sec.) the temperature had become constant.

Fig 6 shows the displacement of the tunnel floor measured at the points shown in Fig 3. Since the time scale is logarithmic the first measurement at zero time is not marked. The first point in the diagram (after 4.75 days) represents the start of the heating period. Fig 6 shows that the rock floor was heaving 1-2 days after start, while it settled in the sub sequent 20-30 days, after which a second heave took place. This latter movement ceased after 100 days and at that time the net average heave was 50 μm.

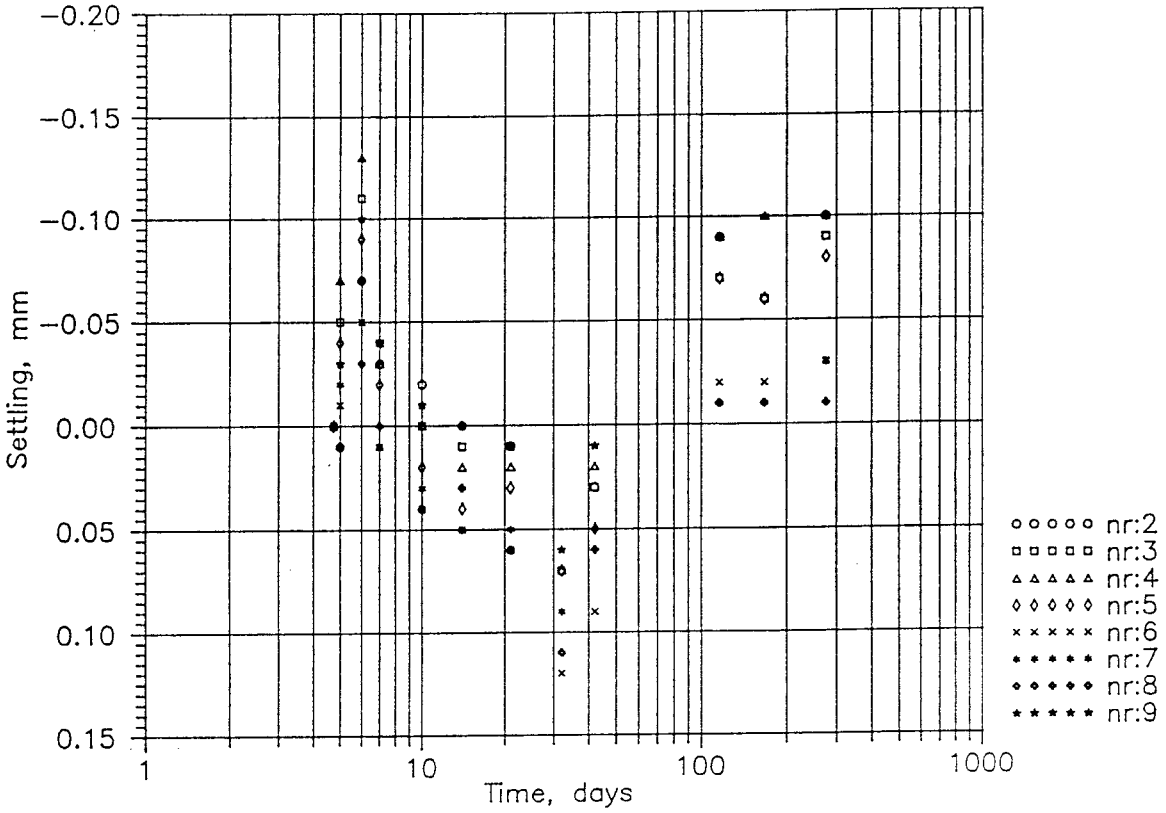

Fig 6. Measured displacements of the tunnel floor. The locations of the measuring points are shown in Fig 3.

4. EVALUATION

In order to try to understand the processes and estimate their respective contribution to the recorded movements, calculations of the water uptake process, the creep settlement, the possible swelling and consolidation processes, the temperature development and the thermomechanical processes have been performed.

4.1 Water uptake

The theoretical ultimate water content of the bentonite was calculated to be 25% and since the initial

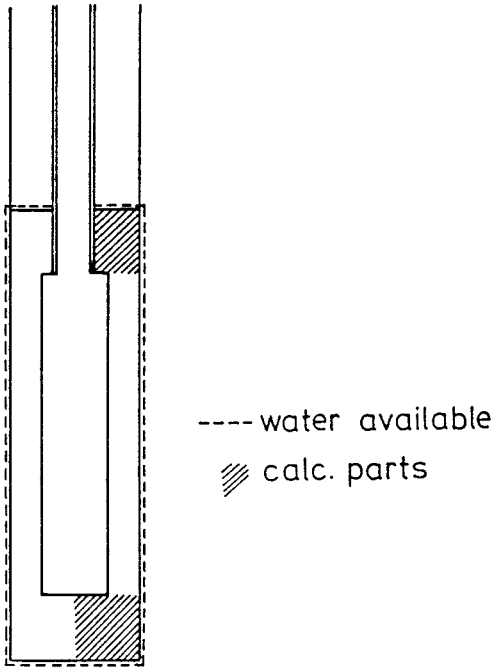

Fig 7. The boundary conditions and the two parts of the bentonite in which the water uptake process is studied.

content was 10%, the uptake would be 15%. The water uptake can be regarded as a diffusion process with the water content difference as driving force and with a coefficient of diffusion of $D_w=0.3\cdot10^{-9}$ m^2/s.

The time for complete saturation is determined by the amount of bentonite below and above the canister. The water uptake process was calculated assuming that enough water is supplied by the rock along the rock surface as well as by the sand/bentonite mixture above and the concrete below the compacted bentonite. The base of the heater cylinder was equipped with a pore pressure device through which the bentonite was wetted and thus the water uptake in the bentonite could be accelerated.

Fig 7 shows the boundary conditions assumed for the calculations which were confined to the two shaded

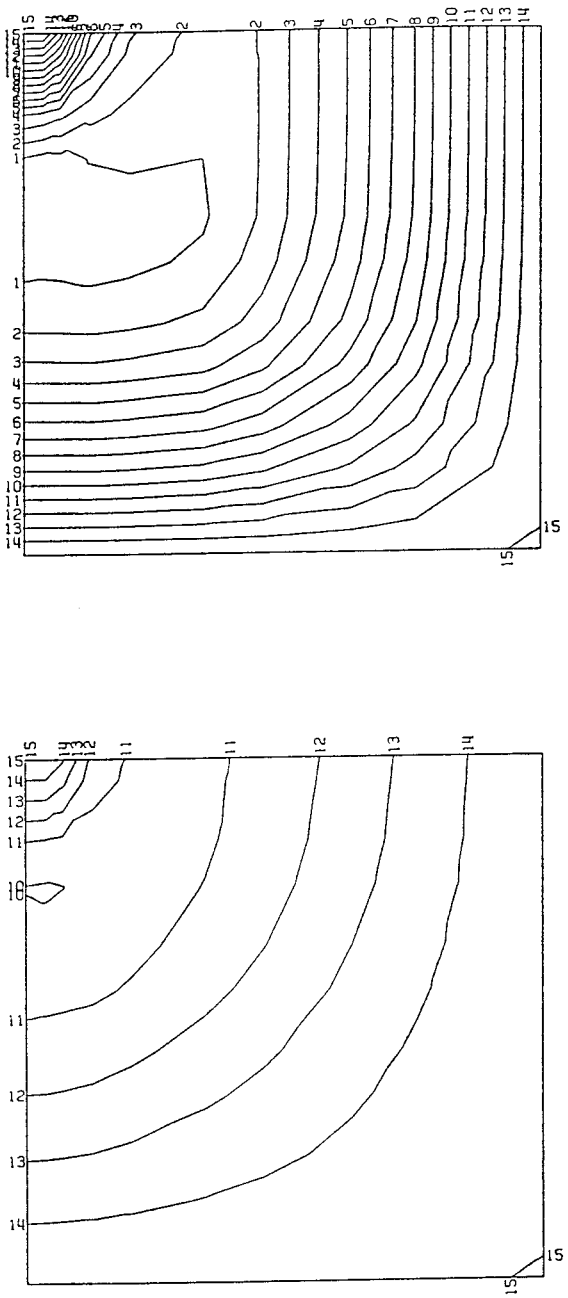

Fig 8. The calculated increase in water ratio below the canister after 56 days (upper) and 270 days. The left side is the axis of rotational symmetry

parts and which were based on axial symmetry conditions. Water was assumed to be supplied along the entire bentonite boundary. The results showed that both parts were saturated simultaneously after about 450 days (>95% saturation everywhere in the bento-

nite). Fig 8 shows the increased water content below the canister after 56 and 270 days, respectively. The real rate of water uptake is uncertain. Since the borehole was core-drilled and since the water pressure in the rock is low due to the surrounding bore holes, it is possible that the assumed boundary conditions are not fulfilled. The water saturation process will in that case be slower than shown by the calculations.

4.2 Creep settlement

The weight of the canister may cause undrained creep settlements due to internal deviatoric stresses in the bentonite. This was investigated by triaxial creep tests and the use of a material model that has been developed and is incorporated in the finite element program ABAQUS.

The creep settlement was calculated for the actual geometry and clay density at different additional loads ΔF (in excess of the load needed for compensating the upward force) varying between 0.71 and 45.0 tons. Fig 9 shows the finite element structure (rotational symmetry) and the deformed clay structure at different times at the applied load ΔF=3.15 t. The settlement is very small, the deformations being enlarged 1 000 times in the graphs.

Fig 10 shows the time-settlement curve for two applied loads and the settlement after 0.5 years and 1 000 years as functions of the applied load. Fig 10 clearly shows that the creep settlements are very small (less than 0.1 mm) at loads similar to those applied in the in situ test. Actually, the load must exceed 50 tons to cause a creep settlement of about one mm. The weight of the canister in the KBS 3 con-

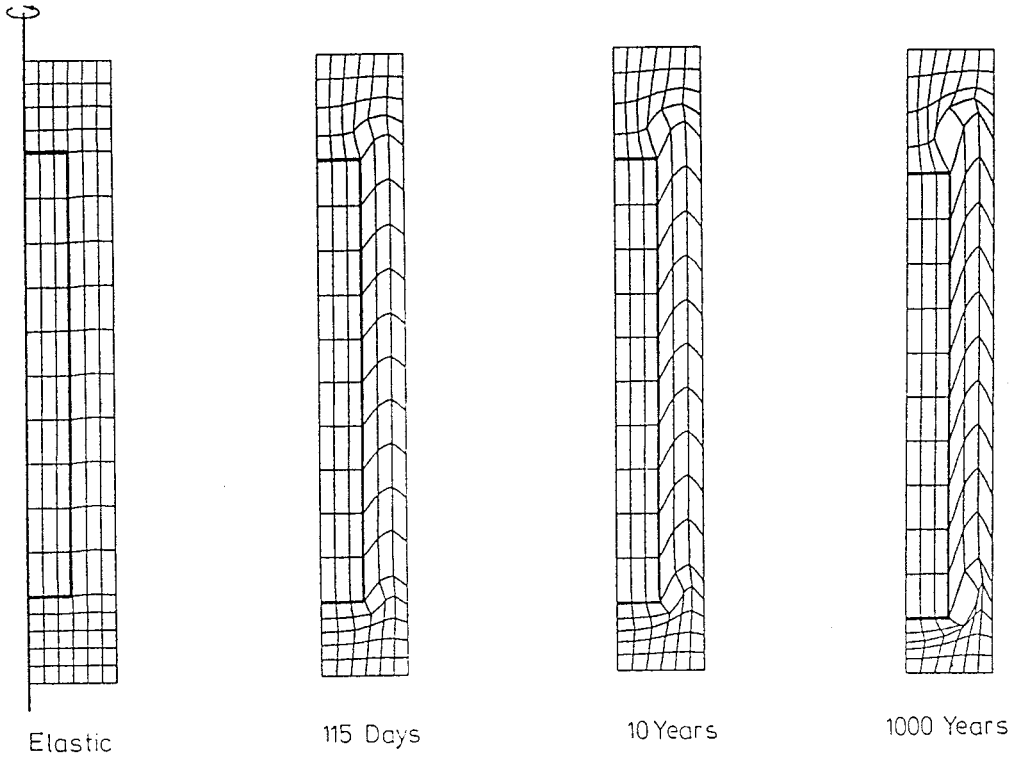

Fig 9. Result of a creep calculation with an applied canister load of 3.15 tons. The displacements are enlarged 1 000 times.

cept corresponds to 1.26 tons in this scale, meaning that the expected settlement of such a canister by undrained creep will be negligible.

The calculated creep settlement can be compared to the measured settlement at the two latest load increments. The net load applied at the last load step was ΔF=7.52-3.14=4.4 t while it amounted to ΔF=3.0 at the last but one. According to the calculations the creep settlement after 50 days would be 0.03-0.04 mm at the corresponding loads but the measured one is 0.10-0.15

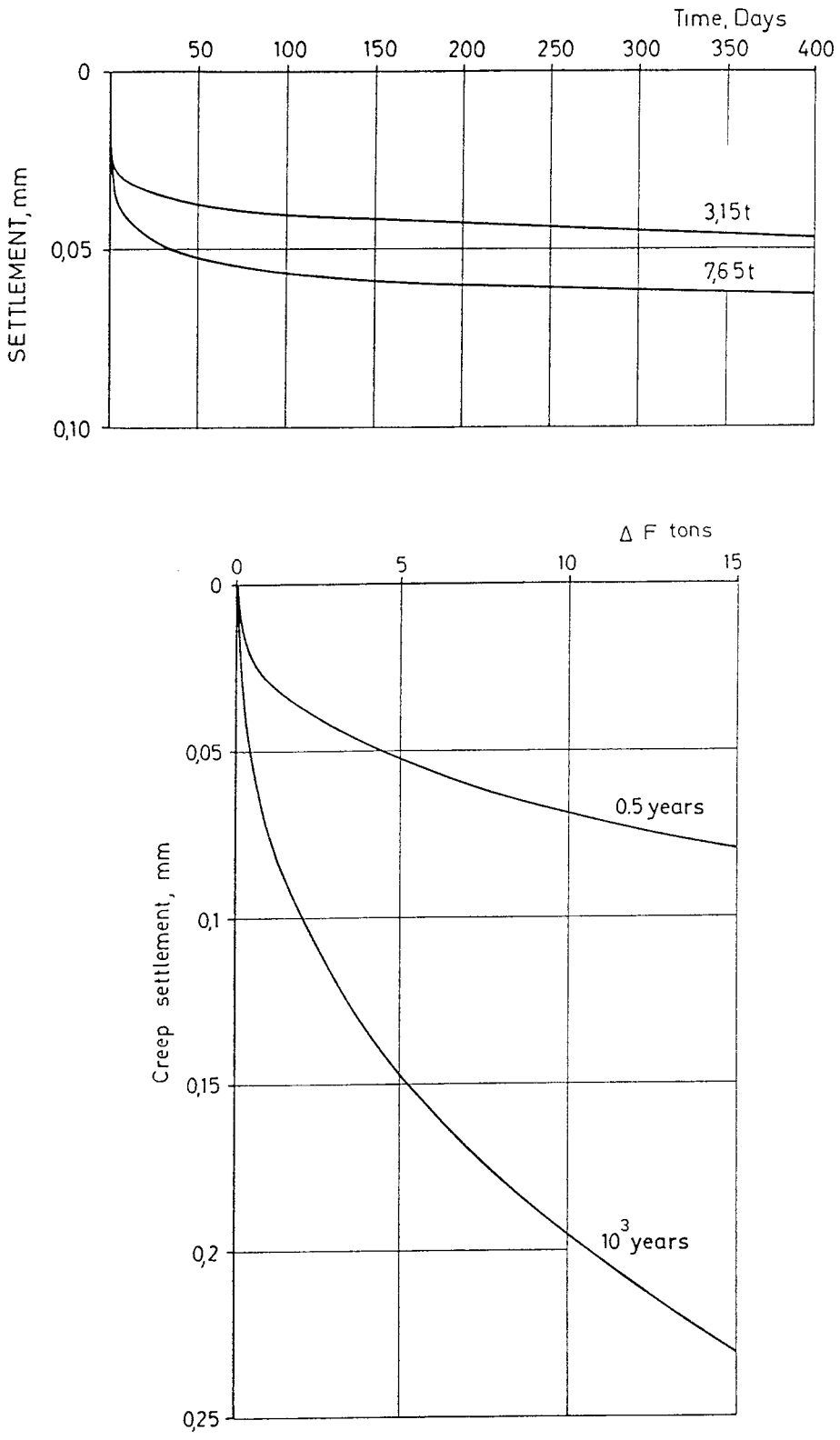

Fig 10. Results of the creep calculations. The upper diagram shows the time-settlement curve for two loads while the lower diagram shows the settlement as a function of the load after 0.5 and 1 000 years.

mm or 3-4 times more despite the continuous heave. This indicates that the consolidation due to the increased average stress is dominating. (cf. Chapter 4.3).

4.3 Consolidation settlement

If the equilibrium between the swelling pressure at the existing void ratio of the clay and the external pressure is changed, e.g. by an increased or decreased load that changes the average stress, a consolidation or swelling process will start. A measure of the amount of volume change that will take place is the void ratio-pressure relation which for Na-bentonite Mx-80 can be written according to Eqn 1.

$$e = 0.165 \cdot \ln(4000/\sigma) + 0.818 \qquad (1)$$

where $\sigma = p$ = swelling pressure or average stress (kPa)

e = void ratio

The rate of consolidation and swelling is determined by the pore pressure dissipation, which, in its turn depends on the coefficient of consolidation c_v and the geometry. Fig 11 shows c_v as a function of the void ratio.

Since the material models for ABAQUS calculations of these processes are not yet available, an estimation based on the change in average stress below the canister must be made. Fig 12 shows the increase in Mises stress q and average stress p caused by a resulting load of ΔF=1.26 t. The figure shows that q is quite small (≈4 kPa) while p has an average value of ≈80 kPa below the canister.

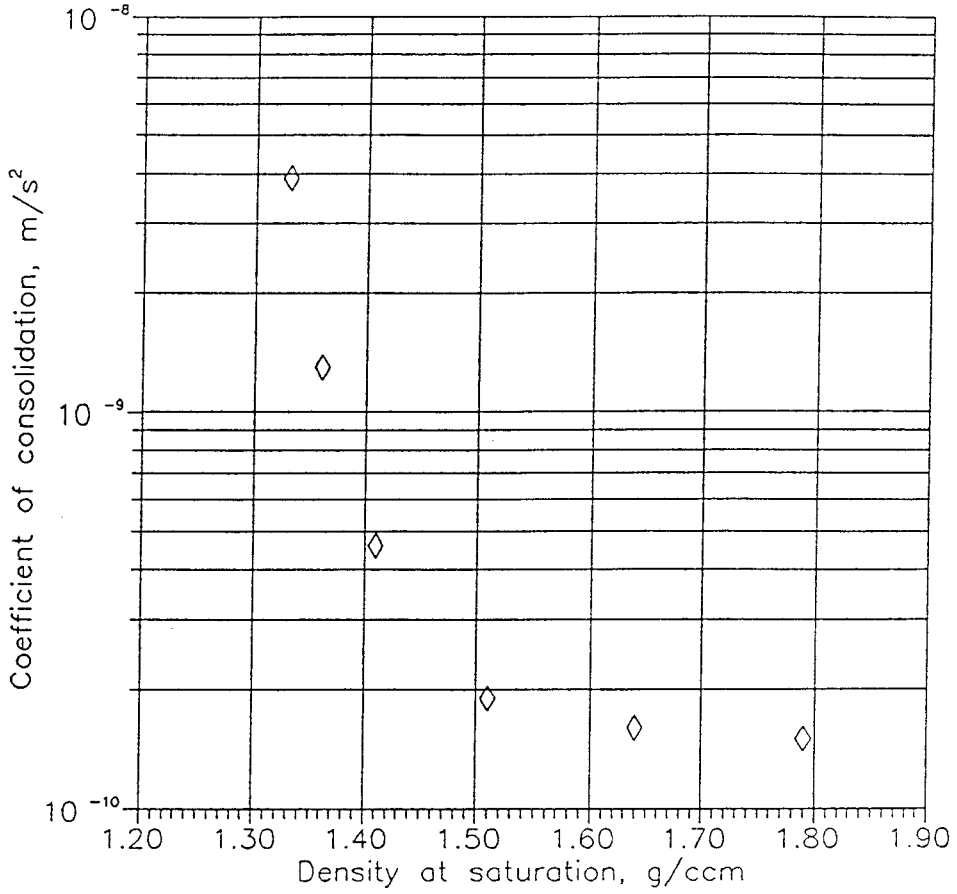

Fig 11. Coefficient of consolidation c_v as a function of the density at saturation ρ_m of Na-smectite clay determined from laboratory tests.

The initial void ratio at ρ_m=1.99 t/m^3 is

$$e = \frac{\rho_s - \rho_m}{\rho_m - \rho_w} = \frac{2.80-1.99}{1.99-1.00} = 0.818 \qquad (2)$$

where ρ_s = particle density
ρ_m = bulk density at saturation
ρ_w = density of pore water

According to Eqn 1 an increased average stress of 80 kPa yields Δe = 0.0033 and a corresponding compression of ε = 0.0018. The thickness of the bentonite below the heater is 0.2 m yielding a consolidation settlement of 0.36 mm. This is 10 times more than the creep settlement after 0.5 years and 4 times more than after 10^4 years.

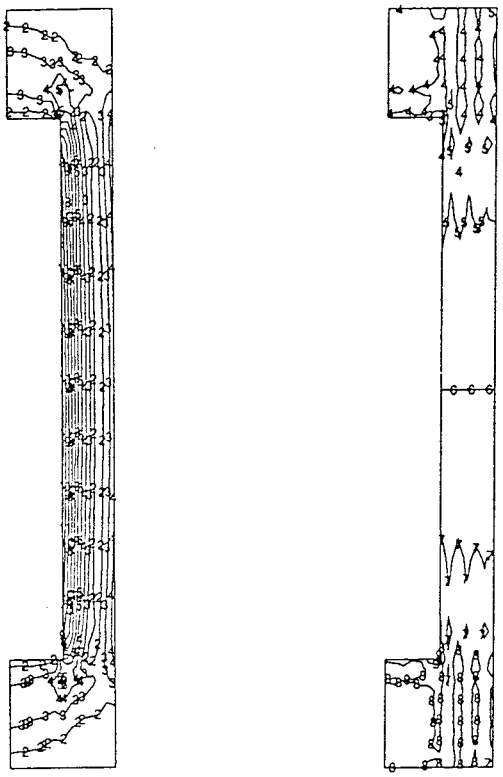

Fig 12. The increase in Mises stress q (left) and average stress p caused by a canister load of 1.26 tons.

Line nr	q kPa	p kPa
1	0	200 (comp.)
2	2	160
3	4	140
4	6	120
Δ	+2	-20

The rate of the consolidation settlement has been determined by FEM calculations using the actual coefficient of consolidation $c_v = 1.0 \cdot 10^{-10}$ m^2/s. The same geometries and boundary conditions have been used as in the water uptake calculations. Fig 13 shows the average degree of consolidation as a function of the elapsed time in days. The figure shows that half the settlement is developed after 75 days while it takes 1 000 days until complete consolidation has taken place (95%).

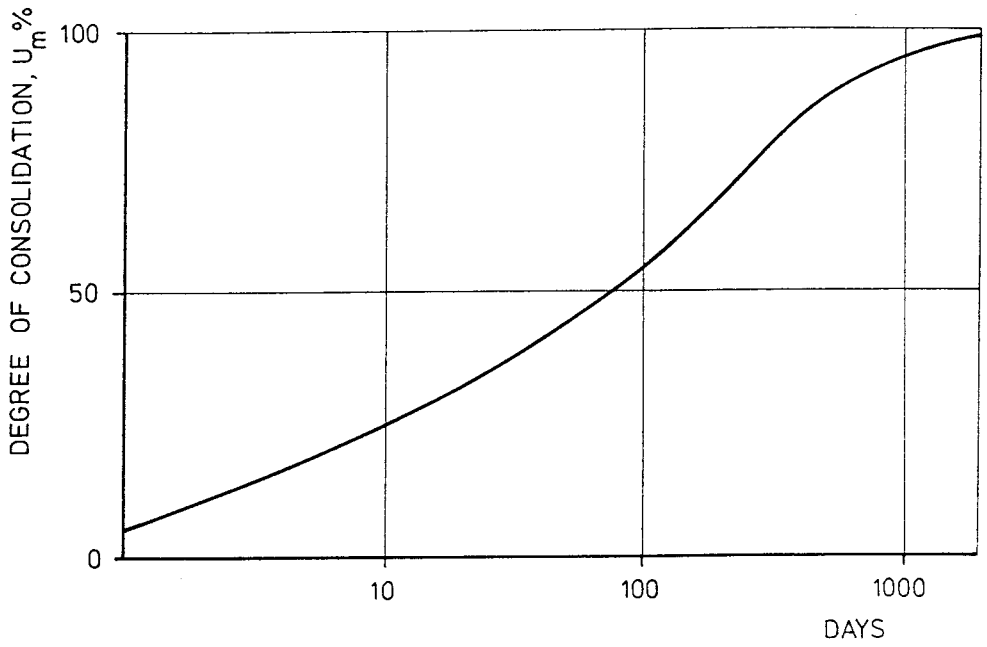

Fig 13. The average degree of consolidation as a function of time for the bentonite below the canister.

The measured settlement after the last load increase can be used for checking the calculations. In doing so, at least four different processes that affect the settlement have to be taken into account:

1. The undrained creep settlement
2. The consolidation settlement from the latest applied load
3. The consolidation settlement from the previous applied loads
4. The heave from the swelling of the compacted bentonite into the sand/bentonite mixture

The creep settlement for the load ΔF = 4.4 t can be estimated from Fig 10. Since this load was not applied in one step, the real creep settlement is somewhat smaller or about 0.04 mm after 50 days.

The last load step was applied 100 days after the preceeding one. According to Fig 13, 55% of the

consolidation/settlement from the previous load increase had been developed after these 100 days and another 7% will be developed in the following 50 days. During these 50 days, 45% of the settlement from the last applied load will be developed. All this means that more than 85% of the measured consolidation/settlement originates from the last load, which amounted to 1.4 tons (cf. Fig. 4). The total settlement from that load increase will be 0.4 mm. After 50 days 45% of the settlement, or 0.18 mm, is achieved.

Setting the preceeding load at 1.4 t, one finds that the corresponding settlement will be 7%, or 0.028 mm, during the same 50 days period.

The slow and steady heave of the canister seems to be about 0.04 mm in 50 days if the displacement curve at 550 days is extrapolated and as much as 0.1 mm in 50 days if the displacement curve at 1 000 days is used. This process will be further dealt with in chapter 4.4.

The displacements from these 4 processes are shown in Fig 14 together with the measured displacement. The two ways of extrapolating the heave are included (curves 4A and 4B) as well as the resulting settlement curves (curves ΣA and ΣB). As can be seen in the figure the measured settlement is intermediate to the two calculated curves. If the heave is supposed to be 0.07 mm in 50 days (4C) the resulting settlement will agree fairly well with the measured one (ΣC). This means that the heave is important for the evaluation and needs to be further studied (cf. Ch. 4.4). It is concluded, however, that the different processes are fairly well understood and that their respective contribution to the net move of the heater can be quantified.

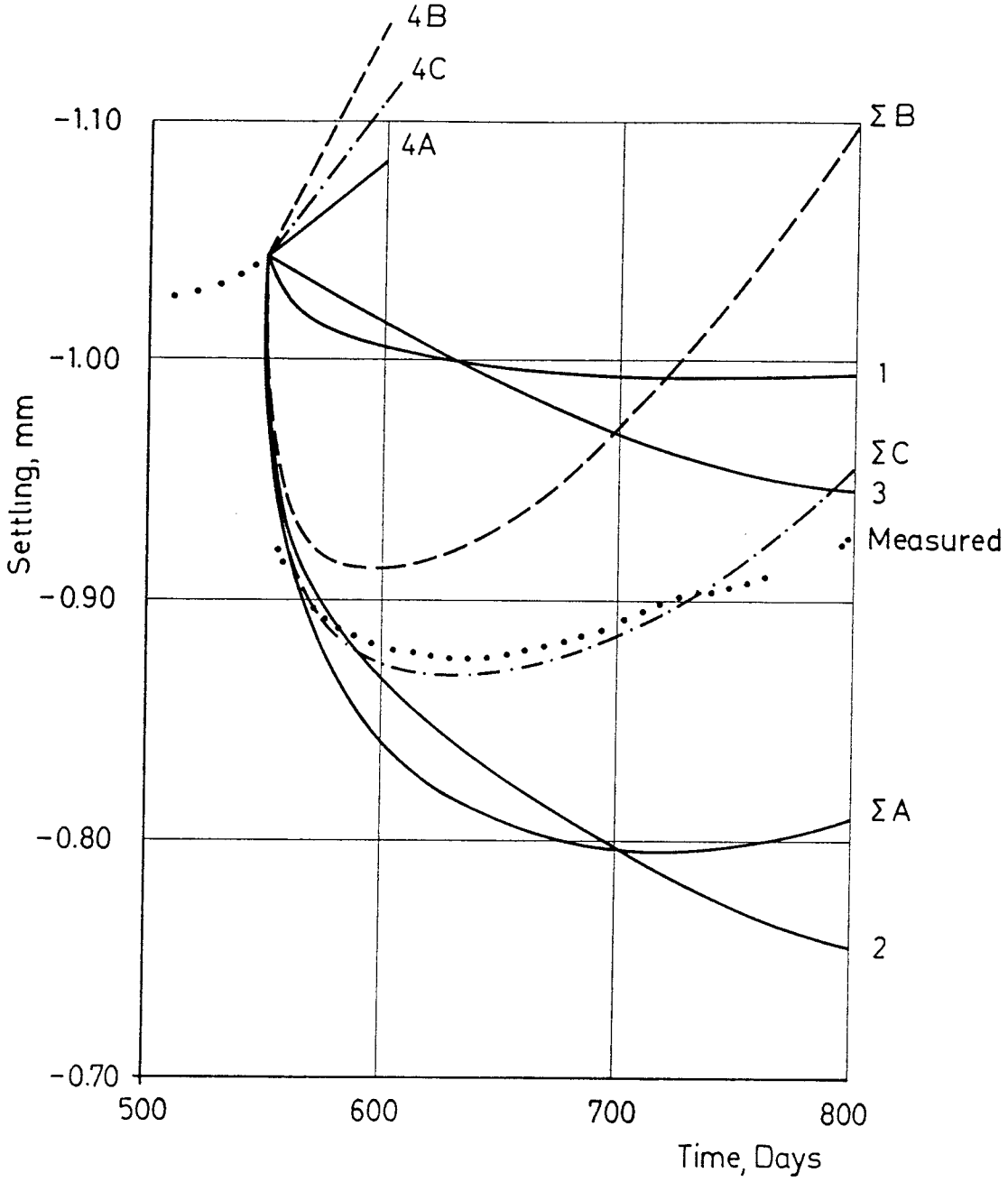

Fig 14. The calculated and measured settlement as a function of time after the latest load increase.

1 = undrained creep

2 = consolidation from the latest load

3 = consolidation from the previous loads

4A, 4B, 4C = heave from swelling

Σ = sum of curves 1-4

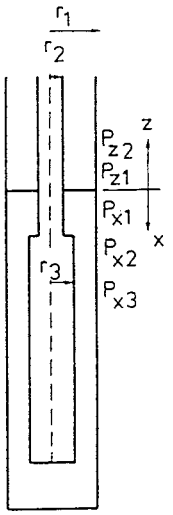

Fig 15. Description of the parameters in Eqn 3 and the subsequent swelling calculations.

4.4 Heave by swelling.

The swelling pressure from the compacted bentonite will cause a compression of the overlying sand/bentonite mixture. The resulting decreased density of the bentonite above and possibly beside the canister will create a resulting pressure upwards due to the difference in swelling pressure above and below the canister. The compression of the sand/bentonite mixture, which is equal to the swelling of the compacted bentonite, can be estimated by a method proposed by Börgesson (1982):

The compression of the sand/bentonite can be calculated at different assumed external pressures p_{z1} exerted at the interface between the sand/bentonite and the compacted bentonite. The stress decrease along the cylinder due to wall friction in a double cylinder with an outer radius r_1 and an inner radius r_2 can be estimated according to Eqn 3 (see Fig 15):

$$\frac{p_{z1}}{p_{z2}} = e^{\frac{2Kz\tan\phi}{r_1 - r_2}} \qquad (3)$$

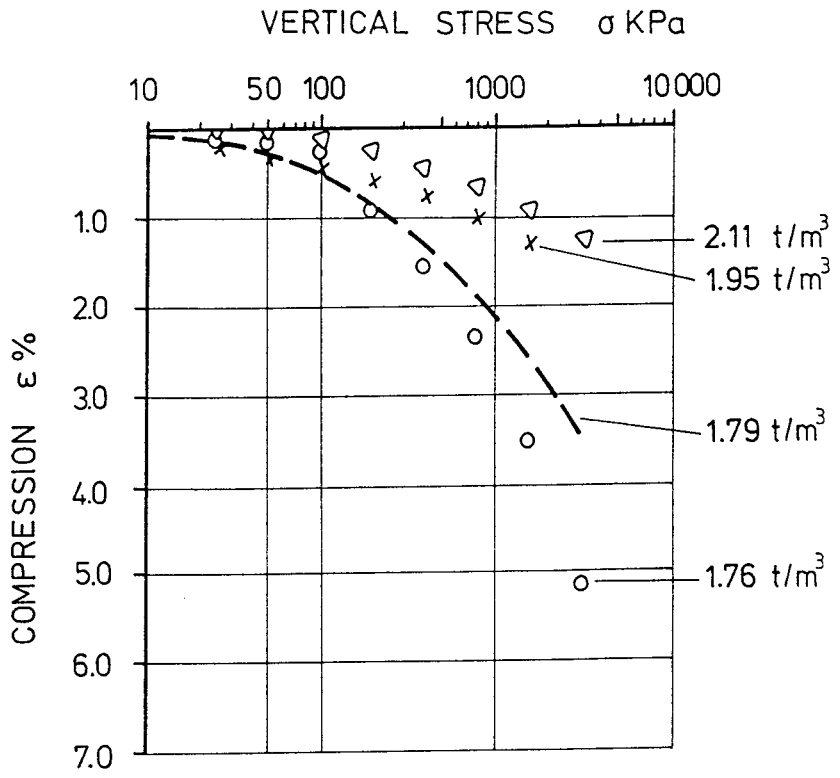

Fig 16. Results from oedometer tests on mixtures of 10% bentonite and 90% sand with different initial dry densities.

where $K = \Delta\sigma_3/\Delta\sigma_1$ at one-dimensional compression and $K = \Delta\sigma_1/\Delta\sigma_3$ at one-dimensional expansion. Using Eqn 3, the vertical stress p_{z2} at the top of the sand/-bentonite can be calculated and thus also the average stress. The compression of the sand/bentonite can then be estimated according to compression curves from laboratory oedometer tests. Fig 16 shows the results from 4 oedometer tests at different initial dry densities.

The expansion of the compacted bentonite can be estimated in a similar way at different external pressures p_{x1} using Eqn 3 and x, p_{x1} and p_{x2} instead of z, p_{z1} and p_{z2}.

Such calculations yield the compression as a function of the pressure p_{z1} and the expansion as a function

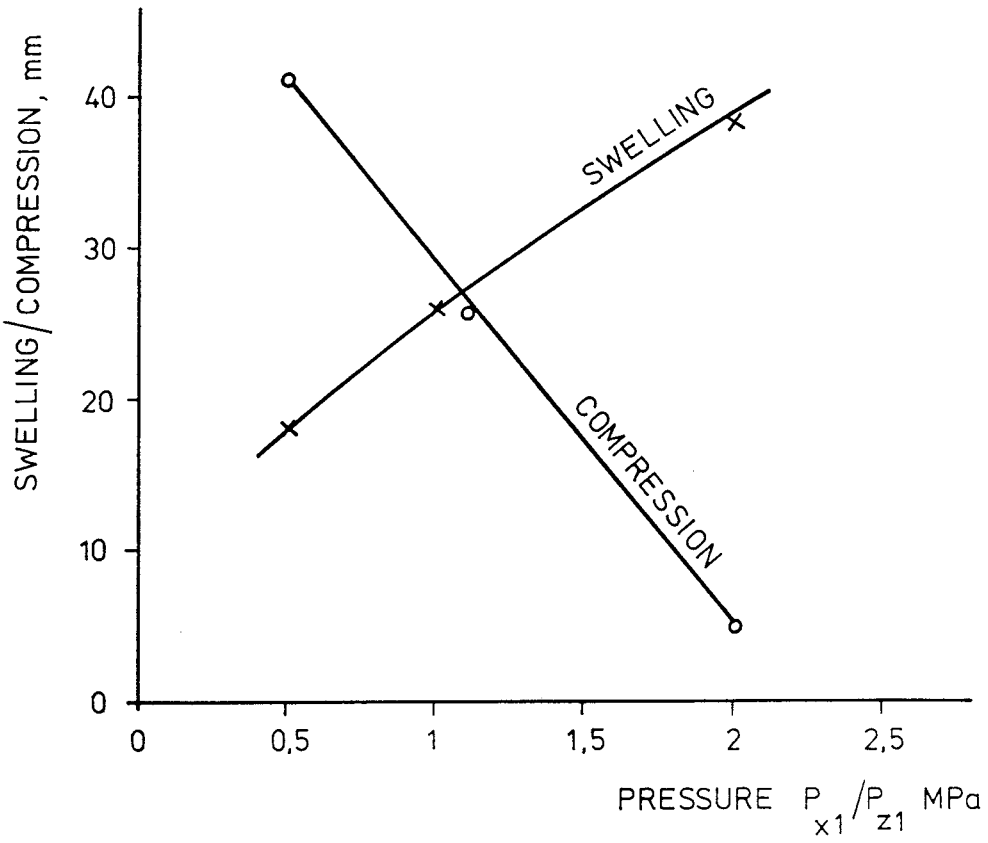

Fig 17. The compression of the sand/bentonite mixture as a function of the pressure p_{z1} and the swelling of the compacted bentonite as a function of the pressure p_{x1}.

of p_{x1}. Since $p_{z1}=p_{x1}$ the intercept between these two relations will yield the actual displacement of the interface.

The initial density of the sand/bentonite is not known but the probable figure ρ_d= 1.75 was assumed in the calculation. The factor K is estimated to be 0.7 at compression and 1.4 at expansion and the friction angle ϕ is approximately 10° at the density ρ_m=2.0 t/m^3.

The swelling is propagating down to the heater and the change in inner radius from r_2 to r_3 must thus be taken into account. Fig 17 shows the result of these calculations. The curves are intercepting at the

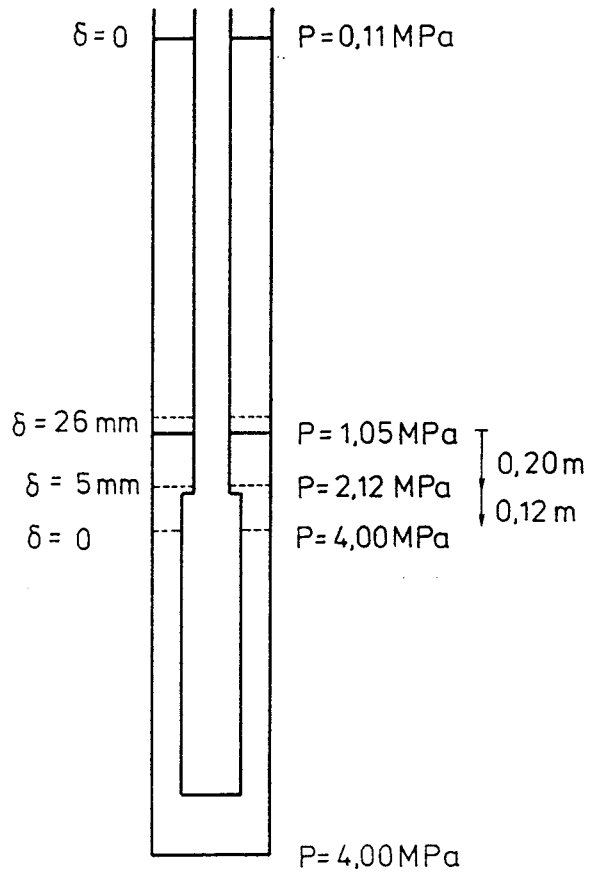

Fig 18. The resulting pressure p and displacement δ derived from the calculations.

displacement 27 mm corresponding to the pressure 1.05 MPa at the interface between the sand/bentonite and the compacted bentonite. The resulting pressure distribution and displacements are shown in Fig 18.

The difference in pressure below and above the heater according to this calculation is 1.88 MPa. The force upwards is thus:

$$F = \pi \cdot (0.1^2 \cdot 4000 - (0.1^2 - 0.06^2) \cdot 2120) = 83 \text{ kN} = 8.3 \text{ t}.$$

The required force to balance the total force upwards is thus higher than the applied one (7.5 t). This means that there is a net force upwards that will result in a heave. However, the measured heave is too large to be explained by the net force 0.8 tons and

this indicates that the initial dry density of the sand/bentonite probably was considerably lower than 1.75 t/m^3.

The required time for complete swelling is dependent on the boundary conditions. If the required amount of water is supposed to be available along the whole periphery of the compacted bentonite, the time for complete swelling of the bentonite above the canister can be calculated in the same way as the consolidation of the bentonite below the canister in Chapter 4.3.

If swelling is considered to be a process of "reverse consolidation"[1] a "coefficient of swelling" c_{sv} similar to the coefficient of consolidation c_v can be evaluated from the laboratory tests accounted for by Börgesson, Hökmark and Karnland (1988). From these tests c_{sv} can be estimated to be $c_{sv} = 1.0 \cdot 10^{-10}$ m/s^2 for densities around $\rho_m = 1.6$ t/m^3. The corresponding values for higher densities can not be evaluated but it will probably be somewhat smaller or $c_{sv} = 0.7\text{-}1.0 \cdot 10^{-10}$ m/s^2. The rate of swelling will thus be similar to the rate of consolidation and the required time for complete swelling (95%) will be 3-4 years.

However, if the supply of water from the surrounding rock is too small, the swelling bentonite must take the required water from the compressed sand/bentonite mixture. This means that the rate of swelling will be slower. A similar calculation yields that the time to complete 95% of the total swelling will be about 13 years under those boundary conditions.

---

[1] A plausible, but not fully validated hypothesis

The total water uptake and swelling should thus be completed in 3-13 years. Today more than 3 years have elapsed since the test was started and the canister is still heaving at a constant rate of 0.1 mm/50 days. This means that the following conclusions can be drawn:

1) The density of the sand/bentonite is probably lower than ρ_d=1.75 t/m^3, which was assumed in the calculation example.

2) At swelling, the bentonite takes its major amount of water required for the swelling from the sand/bentonite mixture.

The swelling process is quite complicated. It involves not only the compression of the sand/bentonite and the swelling of the adjacent bentonite, but also the swelling of the bentonite below the canister and the resulting movement upwards of the heater. An accurate calculation of this process requires complete material models and calculation tools. Such models and tools are under development, and will probably make this calculation possible within a year.

4.5 Thermo-mechanical effects

The temperature of the heater was increased by applying the power 600 W (reduced from 660 W after 13 days). Calculations of the temperature evolution and the thermomechanical consequences have been conducted using ABAQUS. The axi-symmetric element mesh used at these calculations and the different property areas are shown in Fig 19. The material data used are shown in Table I:

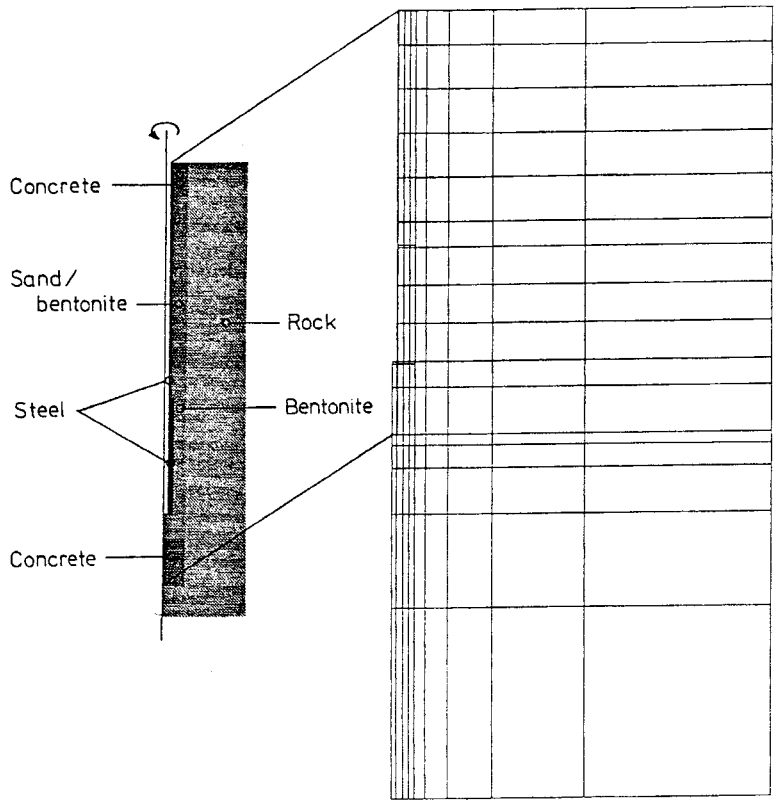

Fig 19. The element mesh and the location of the different materials at the thermomechanical calculations.

TABLE I Material data for the heat and thermomechanical calculations: ρ=density, λ=coefficient of thermal conductivity, c=specific heat, α=coefficient of thermal expansion, E_u=Young's modulus at undrained conditions and E_d=Young's modulus at drained conditions

Material	ρ kg/m^3	λ W/m,°K	c Ws/kg,°K	α 1/°K $*10^{-6}$	E_u Pa $*10^9$	E_d Pa $*10^9$
steel	7700	59	460	12	210	210
concrete	2300	1.8	920	12	30	30
sand/bent.	2100	2.4	1400	200	8	0.01
bentonite	2000	1.4	1600	300	5	0.02
rock	2700	3.6	800	8.3	5	5

The temperature calculation resulted in a stabilized temperature increase of the heater of $\Delta T=77^{\circ}C$ after approximately 100 days. Since the original temperature was $16^{\circ}C$ the total final temperature of the canister will be $93^{\circ}C$. The final temperature of the bentonite/rock interface in the centre plane of the canister will according to these calculations be $53^{\circ}C$.

The measured temperatures were 92 and $94^{\circ}C$ at the canister/bentonite interface and 49 and $50^{\circ}C$ at the bentonite/rock interface. The nice agreement between the calculated and measured values indicates that the bentonite at midheight canister is very close to saturation since the value $\lambda=1.4$ W/m,$^{\circ}K$ correponds to the coefficient of thermal conductivity of compacted water saturated bentonite.

The thermomechanical calculation is more complex. The high coefficent of thermal expansion of the compacted bentonite and the sand/bentonite mixture $\alpha=2\text{-}3*10^{-4}$ $1/^{\circ}K$ in combination with the high Young's modulus at undrained conditions $E=5\text{-}8*10^{9}$ Pa is only valid for a short time. Expansion of the pore water is dominating and a very high pore pressure will be the result of an increased temperature in such a confined system. The pore pressure will drop simultaneously with an outflow of water. This process is similar to the consolidation process, with the exception that the void ratio does not change.

If the particles are considered incompressible and without thermal expansion, only the volume of water corresponding to the final water expansion minus the volume change of the confinement, must leave the clay. It has been shown theoretically as well as by laboratory tests that the corresponding "coefficient of consolidation" at constant volume is $c_p \approx 10^{-8}$ m/s^2. The pore pressure equalization will thus be approxi-

mately 100 times faster than at ordinary consolidation and will be finished in less than 10 days.

The situation after the pore pressure has dropped to the in situ value corresponds to the drained case, which means that E_d in Table I can be used for the thermomechanical calculation. Calculations of the undrained as well as the drained cases have been performed. The results from these calculations differ very much due to the very high stresses in the bentonite at the undrained case. After one week the average stress, calculated at undrained conditions, is ≈50 MPa in the central part of the bentonite, while it is only ≈0.4 MPa, under drained conditions.

The deformed structures after one day, one week and one year have been calculated. After one day the undrained state is dominating. After one week and one year the drained state is valid since the transition from undrained to drained conditions takes place somewhere between 1 day and 1 week. Fig 20 shows the deformed structure after one day (undrained) and one week (drained), respectively.

4.6 Rock movements

The calculated heave of the rock surface was 0.06-0.08 mm after one day (undrained), 0.02-0.03 mm after one week and 0.05-0.06 mm after one year under drained conditions. Fig 21 shows these values plotted together with the measured heave of the rock floor. It is very interesting to note that the general tendency indicated by the calculations, with an initial heave for a couple of days followed by a settlement and a final heave after a long time, agrees very well with the measurements. Even the figures of the measured heave agree quite well with the calculated ones in the first week and after more than 100 days.

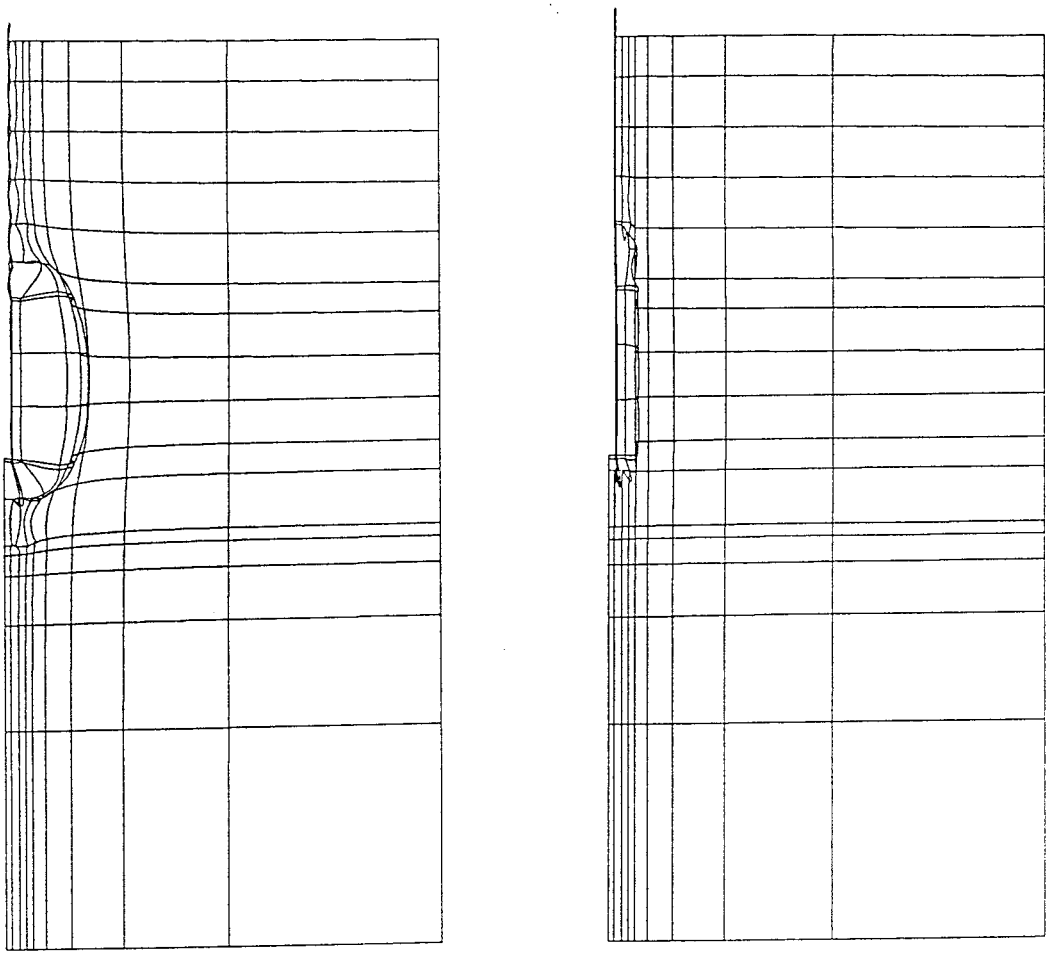

Fig 20. The deformed structure one day (left, undrained) and one week (drained) after start of the heating period. The displacements are enlarged 440 times in the left figure and 390 times in the right.

However, the large settlement that brings the total heave to be negative 10 to 100 days after start can never result from FEM calculations of homogeneous structures. It can only be explained by block movements. A possible scenario that can result in such a settlement is shown in Fig 22. Two blocks A and B have been influenced by the very high internal pressure in the simulated deposition hole caused by the heating of the pore water. At the pressure decrease block B is stuck and does not move back to the ini-

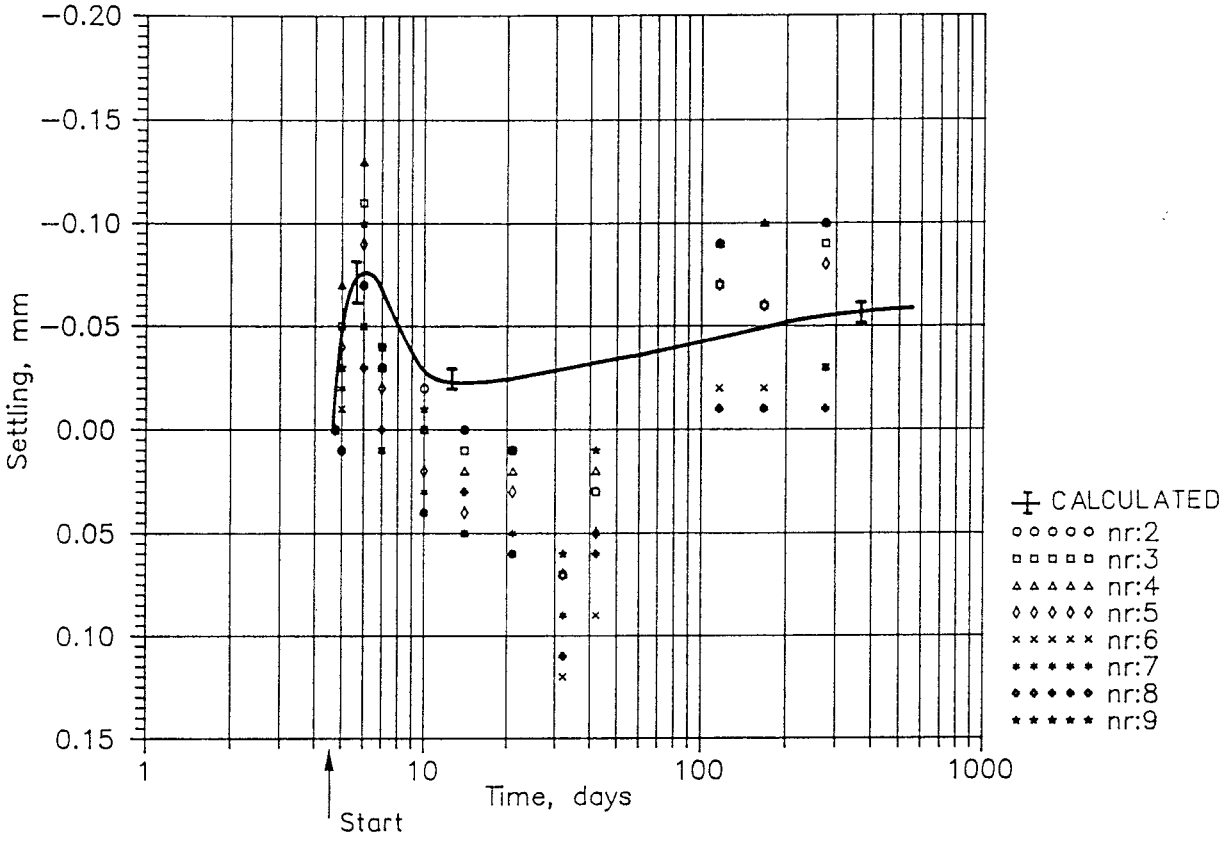

Fig 21. The calculated heave of the tunnel floor, caused by the heat of the canister, as a function of time compared to the measured.

tial position while block A is free to move. Block A will thus move back into the hole and slide downwards. The result can be a final position of block A that is lower than its original position.

Thus the strange rock surface displacements can be explained as a combined effect of high internal pore water pressure in the bentonite caused by the heat, the quick drainage leading to decrease in pressure, and block movements around the simulated deposition hole. $c_p \approx 10^{-8}$ m^2/s that was used in the calculations would yield a time for complete pore pressure equilization of approximately 10 days as shown in Fig 21, but the measured displacements indicate that the drainage is somewhat slower (20-40 days), which may be due to either that c_p is a little lower or that the drainage is delayed by resistance from the rock.

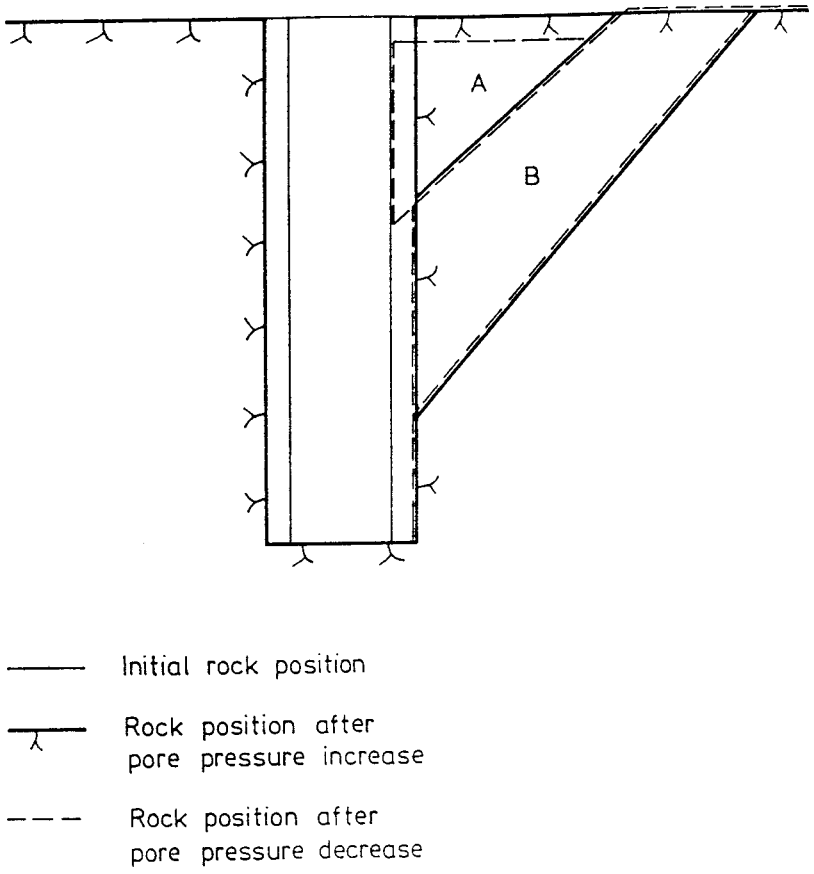

Fig 22. A scenario in which the tunnel floor can settle as a result of an applied high temperature in a deposition hole. The induced high pore pressure in the bentonite will expand the hole. After pore pressure equilization block B is stuck while block A is sliding downwards.

The measurements and calculations also support the conclusion that the clay is highly saturated.

5. CONCLUSIONS

The main conclusions that can be drawn from the test and performed calculations are, so far, the following ones:

A. The bentonite is probably highly saturated
B. The creep settlement is small
C. The settlement from consolidation is several times larger than the creep settlement
D. The density of the sand-bentonite mixture above the compacted bentonite is probably very low. Due to that low density the compacted bentonite swells upwards, which is the reason for the continuous heave of the canister.
E. The displacement of the tunnel floor after applied heat can be explained by thermomechanical calculations if the block structure of the rock is taken into consideration.
F. The fair agreement between recorded and calculated strain indicates that the various material models used in the calculations are valid.

6. RECOMMENDATIONS FOR FURTHER WORK

Since the canister is still heaving, probably due to the swelling of the compacted bentonite, it is of no use to wait for equilibrium. It is possible to apply another load of 4.5 tons on the heater which will lead to a total load of 12 tons. This load should be applied on November 1, 1989 in order to study the response of the heated system and compare it to the measured responses of the unheated system. The resulting settlement should be studied for about half a year and on May 2, 1990, the heat should be turned off.

The response of the canister and the rock to the decreased temperature can then be studied. After a cooling period of three months, the canister should be unloaded on August 1, 1990 and after another six months, on February 4, 1991 the test should be finished and the bentonite excavated.

7. PREDICTION OF THE SETTLEMENT CAUSED BY THE PROPOSED LOAD INCREASE

The settlement will be calculated as the sum of four different processes as shown in Fig 14.

A. Heave by swelling.

The continuous average measured heave is 0.09 mm/50 days. This heave is assumed to continue throughout the whole test. Curve 4 in Fig 23 shows the heave as a function of time.

B. Creep settlement.

The resulting creep settlement can be evaluated from the calculations shown in Fig 10. Since the load is increased from 7.5 to 12 tons, the creep curve related to the load 12 tons cannot be used. Instead the result of the load increase is assumed to be the creep curve from the lower load, subtracted from the creep curve from the higher load which is in agreement with the finding that the creep rate of a load applied in one step is the sum of the creep rates, should the load have been applied in several steps (Börgesson et al 1987). Curve 1 in Fig 23 shows the creep settlement evaluated in this way.

C. Consolidation from the proposed load load increase.

An increase in load of ΔF=4.5 tons means an increase in average stress $\Delta p \approx 290$ kPa according to Fig 12 since the stresses are proportional to the load. This leads to a decrease in void ratio Δe=0.0115 according to Eqn 1. The settlement at 100% degree of consolidation, resulting from the decrease in void ratio, will be 2.31 mm since the compacted bentonite below the heater is 0.2 m thick.

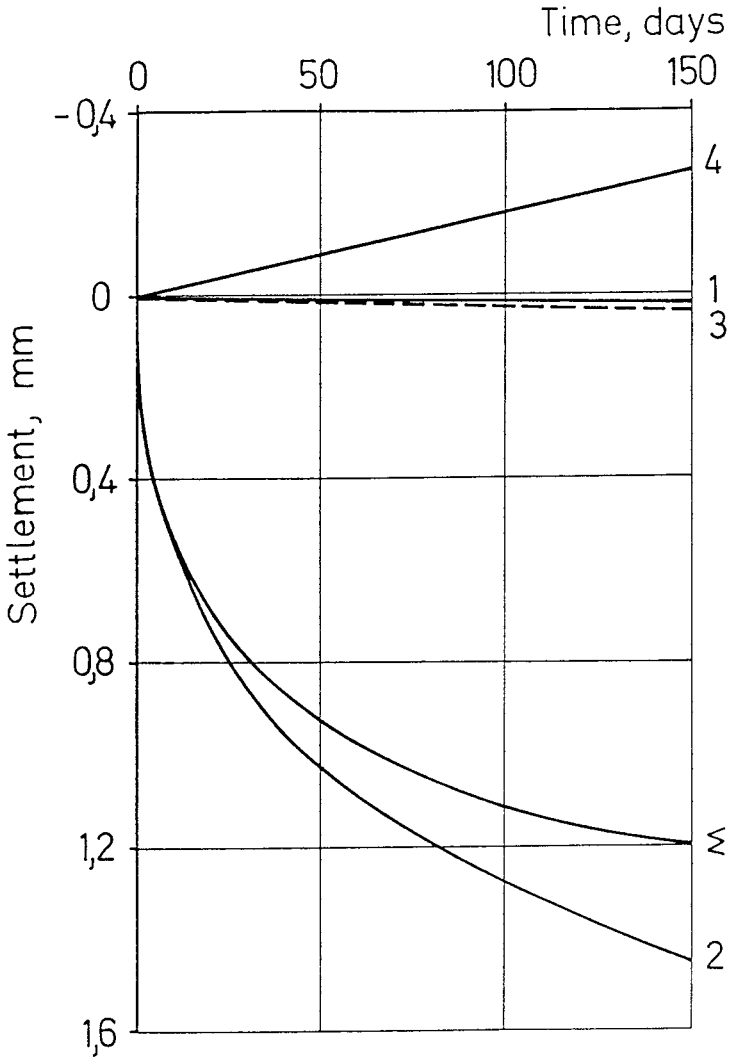

Fig 23. The prediced settlement as a function of time after the proposed load increase from 7.5 to 12 t

1 = undrained creep

2 = consolidation from the proposed load increase

3 = consolidation from the previous loads

4 = present heave

Σ = resulting settlement

The rate of the settlement is evaluated from Fig 13. Curve 2 in Fig 23 shows the result.

D. Consolidation from earlier loads.

All earlier applied loads can be approximated to a net load of 4.4 tons which is applied about 440 days after start or on September 1, 1987. Since the proposed load increase is going to take place on November 1, 1989, about 790 days will have elapsed since these 4.4 tons were applied. This means that 93% of the settlement is completed. During the next 150 days a settlement of 1.5% or 0.035 mm will take place. Curve 3 in Fig 23 shows the settlement caused by these early loads.

However, this settlement is already included in the heave (curve 4) and it is not necessary to take it into account, unless the change in settlement rate is considerable.

E. Resulting settlement.

The resulting settlement is shown in Fig 23 as curve Σ. The total predicted settlement after about half a year is thus 1.2 mm.

There are two uncertainties in the calculation of the consolidation. The major uncertainty is that the hysteresis effects at loading and unloading has not been taken into account. This effect could decrease the settlement by as much as 50%. The other uncertainty is the possible effect of the increased temperature, since the calculation is based on data from laboratory tests at room temperature. This effect is probably uncertain but can be as high as the hysteresis effect.

REFERENCES

Börgesson, L. 1982. BUFFER MASS/TEST - Predictions of the behaviour of the bentonite-based buffer materials. Stripa Project Internal Report 82-08

Börgesson, L. & Stenman, U. 1985. Laboratory determined properties of sand/bentonite mixtures for WP-cave. Internal report SGAB IRAP 85511

Börgesson, L. 1985. Water flow and swelling pressure in non-saturated bentonite-based clay barriers. Eng. Geol. 21:229-237

Börgesson, L. & Pusch, R. 1987. Rheological properties of a calcium smectite. SKB Technical Report 87-31.

Börgesson, L. 1988. Modelling of buffer material behaviour. Some examples of material models and performance calculations. SKB Technical Report 88-29.

Börgesson, L., Hökmark, H. & Karnland, O. 1988. Rheological properties of sodium smectite clay. SKB Technical Report 88-30.

Graham, J., Sadat, F., Gray, M.N., Dixon, D.A. & Zhang, Q-Y. 1989. Strength and volume change behaviour of a sand-bentonite mixture. Canadian Geotechnical Journal, 26.

Hibbitt, Karlsson and Sorensen. ABAQUS users' manual.

Lambe, T.W. & Whitman, R.V. 1969. Soil Mechanics. John Wiley & Sons, Inc.

Pusch, R. 1983. Stress/strain/time properties of highly compacted bentonite. SKB/KBS Technical Report 83-47.

List of SKB reports

Annual Reports

1977–78
TR 121
KBS Technical Reports 1 – 120.
Summaries. Stockholm, May 1979.

1979
TR 79–28
The KBS Annual Report 1979.
KBS Technical Reports 79-01 – 79-27.
Summaries. Stockholm, March 1980.

1980
TR 80–26
The KBS Annual Report 1980.
KBS Technical Reports 80-01 – 80-25.
Summaries. Stockholm, March 1981.

1981
TR 81–17
The KBS Annual Report 1981.
KBS Technical Reports 81-01 – 81-16.
Summaries. Stockholm, April 1982.

1982
TR 82–28
The KBS Annual Report 1982.
KBS Technical Reports 82-01 – 82-27.
Summaries. Stockholm, July 1983.

1983
TR 83–77
The KBS Annual Report 1983.
KBS Technical Reports 83-01 – 83-76
Summaries. Stockholm, June 1984.

1984
TR 85–01
Annual Research and Development Report 1984
Including Summaries of Technical Reports Issued during 1984. (Technical Reports 84-01–84-19)
Stockholm June 1985.

1985
TR 85-20
Annual Research and Development Report 1985
Including Summaries of Technical Reports Issued during 1985. (Technical Reports 85-01-85-19)
Stockholm May 1986.

1986
TR 86-31
SKB Annual Report 1986
Including Summaries of Technical Reports Issued during 1986
Stockholm, May 1987

1987
TR 87-33
SKB Annual Report 1987
Including Summaries of Technical Reports Issued during 1987
Stockholm, May 1988

1988
TR 88-32
SKB Annual Report 1988
Including Summaries of Technical Reports Issued during 1988
Stockholm, May 1989

Technical Reports

1989
TR 89-01
Near-distance seismological monitoring of the Lansjärv neotectonic fault region Part II: 1988
Rutger Wahlström, Sven-Olof Linder, Conny Holmqvist, Hans-Edy Mårtensson
Seismological Department, Uppsala University, Uppsala
January 1989

TR 89-02
Description of background data in SKB database GEOTAB
Ebbe Eriksson, Stefan Sehlstedt
SGAB, Luleå
February 1989

TR 89-03
Characterization of the morphology, basement rock and tectonics in Sweden
Kennert Röshoff
August 1988

TR 89-04
SKB WP-Cave Project
Radionuclide release from the near-field in a WP-Cave repository
Maria Lindgren, Kristina Skagius
Kemakta Consultants Co, Stockholm
April 1989

TR 89-05
SKB WP-Cave Project
Transport of escaping radionuclides from the WP-Cave repository to the biosphere
Luis Moreno, Sue Arve, Ivars Neretnieks
Royal Institute of Technology, Stockholm
April 1989

TR 89-06
SKB WP-Cave Project
Individual radiation doses from nuclides contained in a WP-Cave repository for spent fuel
Sture Nordlinder, Ulla Bergström
Studsvik Nuclear, Studsvik
April 1989

TR 89-07
SKB WP-Cave Project
Some Notes on Technical Issues
Part 1: Temperature distribution in WP-Cave: when shafts are filled with sand/water mixtures
Stefan Björklund, Lennart Josefson
Division of Solid Mechanics, Chalmers University of Technology, Gothenburg, Sweden
Part 2: Gas and water transport from WP-Cave repository Luis Moreno, Ivars Neretnieks
Department of Chemical Engineering, Royal Institute of Technology, Stockholm, Sweden
Part 3: Transport of escaping nuclides from the WP-Cave repository to the biosphere. Influence of the hydraulic cage
Luis Moreno, Ivars Neretnieks
Department of Chemical Engineering, Royal Institute of Technology, Stockholm, Sweden
August 1989

TR 89-08
SKB WP-Cave Project
Thermally incuded convective motion in groundwater in the near field of the WP-Cave after filling and closure
Polydynamics Limited, Zürich
April 1989

TR 89-09
An evaluation of tracer tests performed at Studsvik
Luis Moreno[1], Ivars Neretnieks[1], Ove Landström[2]
[1] The Royal Institute of Technology, Department of Chemical Engineering, Stockholm
[2] Studsvik Nuclear, Nyköping
March 1989

TR 89-10
Copper produced from powder by HIP to encapsulate nuclear fuel elements
Lars B Ekbom, Sven Bogegård
Swedish National Defence Research Establishment
Materials department, Stockholm
February 1989

TR 89-11
Prediction of hydraulic conductivity and conductive fracture frequency by multivariate analysis of data from the Klipperås study site
Jan-Erik Andersson[1], Lennart Lindqvist[2]
[1] Swedish Geological Co, Uppsala
[2] EMX-system AB, Luleå
February 1988

TR 89-12
Hydraulic interference tests and tracer tests within the Brändan area, Finnsjön study site
The Fracture Zone Project – Phase 3
Jan-Erik Andersson, Lennart Ekman, Erik Gustafsson, Rune Nordqvist, Sven Tirén
Swedish Geological Co, Division of Engineering Geology
June 1988

TR 89-13
Spent fuel
Dissolution and oxidation
An evaluation of literature data
Bernd Grambow
Hanh-Meitner-Institut, Berlin
March 1989

TR 89-14
The SKB spent fuel corrosion program
Status report 1988
Lars O Werme[1], Roy S Forsyth[2]
[1] SKB, Stockholm
[2] Studsvik AB, Nyköping
May 1989

TR 89-15
Comparison between radar data and geophysical, geological and hydrological borehole parameters by multivariate analysis of data
Serje Carlsten, Lennart Lindqvist, Olle Olsson
Swedish Geological Company, Uppsala
March 1989

TR 89-16
Swedish Hard Rock Laboratory – Evaluation of 1988 year pre-investigations and description of the target area, the island of Äspö
Gunnar Gustafsson, Roy Stanfors, Peter Wikberg
June 1989

TR 89-17
Field instrumentation for hydrofracturing stress measurements
Documentation of the 1000 m hydrofracturing unit at Luleå University of Technology
Bjarni Bjarnason, Arne Torikka
August 1989

TR 89-18
Radar investigations at the Saltsjötunnel – predicitions and validation
Olle Olsson[1] and Kai Palmqvist[2]
[1] Abem AB, Uppsala, Sweden
[2] Bergab, Göteborg
June 1989

TR 89-19
Characterization of fracture zone 2, Finnsjön study-site
Editors: K. Ahlbom, J.A.T. Smellie, Swedish Geological Co, Uppsala
Part 1: Overview of the fracture zone project at Finnsjön, Sweden
K. Ahlbom and J.A.T. Smellie. Swedish Geological Company, Uppsala, Sweden.
Part 2: Geological setting and deformation history of a low angle fracture zone at Finnsjön, Sweden
Sven A. Tirén. Swedish Geological Company, Uppsala, Sweden.
Part 3: Hydraulic testing and modelling of a low-angle fracture zone at Finnsjön, Sweden
J-E. Andersson[1], L. Ekman[1], R. Nordqvist[1] and A. Winberg[2]
[1] Swedish Geological Company, Uppsala, Sweden
[2] Swedish Geological Company, Göteborg, Sweden
Part 4: Groundwater flow conditions in a low angle fracture zone at Finnsjön, Sweden
E. Gustafsson and P. Andersson. Swedish Geological Company, Uppsala, Sweden
Part 5: Hydrochemical investigations at Finnsjön, Sweden
J.A.T. Smellie[1] and P. Wikberg[2]
[1] Swedish Geological Company, Uppsala, Sweden
[2] Swedish Nuclear Fuel and Waste Management Company, Stockholm, Sweden
Part 6: Effects of gas-lift pumping on hydraulic borehole conditions at Finnsjön, Sweden
J-E- Andersson, P. Andersson and E. Gustafsson. Swedish Geological Company, Uppsala, Sweden
August 1989

TR 89-20
WP-Cave - Assessment of feasibility, safety and development potential
Swedish Nuclear Fuel and Waste Management Company, Stockholm, Sweden
September 1989

TR 89-21
Rock quality designation of the hydraulic properties in the near field of a final repository for spent nuclear fuel
Hans Carlsson[1], Leif Carlsson[1], Roland Pusch[2]
[1] Swedish Geological Co, SGAB, Gothenburg, Sweden
[2] Clay Technology AB, Lund, Sweden
June 1989

TR 89-22
Diffusion of Am, Pu, U, Np, Cs, I and Tc in compacted sand-bentonite mixture
Department of Nuclear Chemistry, Chalmers University of Technology, Gothenburg, Sweden
August 1989

TR 89-23
Deep ground water microbiology in Swedish granitic rock and it's relevance for radionuclide migration from a Swedish high level nuclear waste repository
Karsten Pedersen
University of Göteborg, Department of Marine microbiology, Gothenburg, Sweden
March 1989

TR 89-24
Some notes on diffusion of radionuclides through compacted clays
Trygve E Eriksen
Royal Institute of Technology, Department of Nuclear Chemistry, Stockholm, Sweden
May 1989

TR 89-25
Radionuclide sorption on crushed and intact granitic rock
Volume and surface effects
Trygve E Eriksen, Birgitta Locklund
Royal Institute of Technology, Department of Nuclear Chemistry, Stockholm, Sweden
May 1989

TR 89-26

Performance and safety analysis of WP-Cave concept

Kristina Skagius[1], Christer Svemar[2]
[1] Kemakta Konsult AB
[2] Swedish Nuclear Fuel and Waste Management Co
August 1989

TR-89-27

Post-excavation analysis of a revised hydraulic model of the Room 209 fracture, URL, Manitoba, Canada
A part of the joint AECL/SKB characterization of the 240 m level at the URL, Manitoba, Canada

Anders Winberg[1], Tin Chan[2], Peter Griffiths[2], Blair Nakka[2]
[1] Swedish Geological Co, Gothenburg, Sweden
[2] Computations & Analysis Section, Applied Geoscience
Branch, Atomic Energy of Canada Limited, Pinawa, Manitoba, Canada
October 1989

TR 89-28

Earthquake mechanisms in Northern Sweden Oct 1987 — Apr 1988

Ragnar Slunga
October 1989